Real Time Control of Shake Tables for Nonlinear Hysteretic Systems

Ki P. Ryu[1]*, Andrei M. Reinhorn[2]

[1,2] *University at Buffalo, State University of New York, USA*

ABSTRACT

Shake table testing is an important tool to challenge integrity of structural and non-structural specimens by imposing excitations at their base. When shake tables are loaded with specimens, the interaction between the tables and specimens influence the system dynamics that result in undesired performance. Open loop feedforward compensation methods have been used successfully in current practice of table controls, assuming that the specimens remain linear. However, unsatisfactory signal performances were observed when flexible and heavy specimens experience nonlinear behavior. While lack of high fidelity might be acceptable for the purpose of exploration of specimens subjected to random excitations, a high fidelity of signal reproduction is necessary for shake table qualification testing where specific target motion is required to challenge the specimens. A nonlinear tracking control scheme based on the feedback linearization method is proposed for the control of shake tables to simulate target motions at specific locations of the test structures having nonlinear hysteretic behavior. A real-time estimator using the extended Kalman filter combined with the controller is adopted in order to account for the changes and uncertainties in system models due to nonlinearities and yielding. The proposed adaptive tracking control method is applied in numerical simulations to a setup of a realistic shake table testing of a nonlinear structure. ,

Keywords: *Shake table test, Nonlinear hysteretic system, Adaptive control, Real-time parameter estimation.*

1 INTRODUCTION

Shake table systems play a pivotal role in the experimental earthquake engineering. The systems provide effective ways to subject structural components, substructures, or entire structural systems to dynamic excitations, which are similar to those induced by real earthquakes [1]-[3]. Unlike general shake table testing where it is required to simulate a desired target motion at the shake table level, in other applications including the experimental evaluation of architectural or non-structural components such as suspended ceiling systems [4] or the qualification testing of complex equipment [5] it is often required to simulate a floor/roof motion at a specific location (such as roof corners or mid spans) of a structure mounted on a shake table. In order to simulate a target motion at a structure level (instead of the shake table platform), a feedforward compensation procedure using a shake table-structure system transfer function with possible offline iteration correction was developed, and the control method was verified experimentally [6].

The key element, for the development of tracking control methods for shake table discussed above, is a feedforward compensation method using the inverse transfer function. However, if a testing structure has more complex, nonlinear behavior (e.g. base-isolated systems) or a linear structure experiences yielding due to high intensity excitation, the transfer function, which can be defined only for a linear time invariant system [7], is not valid anymore. Therefore, the feedforward compensation loop, which is conducted offline, cannot be used and real-time feedback control schemes are needed [6].

[1] Post Doctoral Research Scientist, kipung@gmail.com

[2] Professor Emeritus, reinhorn@buffalo.edu

* Corresponding author

The objective of this study is to simulate a target motion at a specific location in a nonlinear structure mounted on a shake table for extended applications such as the qualification testing addressed above. To solve this tracking control problem, a real-time nonlinear feedback control scheme based on the feedback linearization method [8], [9] is proposed. A difficult challenge for a nonlinear structure control is that the system parameters might not be known a priori; for example, the change of structure stiffness in hysteretic behavior and/or the yielding force may not be accurately known in advance. In these cases, a real-time parameter estimation method might be required for adaptive control schemes. As addressed above, in this study, a real-time nonlinear feedback tracking controller based on the feedback linearization method is formulated and combined with the extended Kalman filter [10]-[12] as a real-time state and parameter estimator in order to develop a methodology to determine the control excitation input of a shake table, such that the output response of a nonlinear hysteretic structure will follow a pre-defined target motion.

2 SHAKE TABLE – NONLINEAR HYSTERETIC STRUCTURE SYSTEM MODEL

A shake table-structure system consists of a platform supported by bearings driven by servo controlled actuators and a structure (specimen) mounted rigidly on its surface. The simplified schematic of the assembly of the shake table–structure system is shown in Figure 1 where actuators' forces and internal stress resultants acting on the system are also presented (i.e. $f_{s,I}$, f_D, f_S are the structure inertia, damping, and restoring forces; $f_{t,I}$ is the table inertia force; f_a is the actuator force). x_t is the shake table displacement with respect to the ground, and x_s is the relative displacement at the top of the structure with respect to the shake table. m_t and m_s are the mass of the shake table and the mass of the structure, respectively.

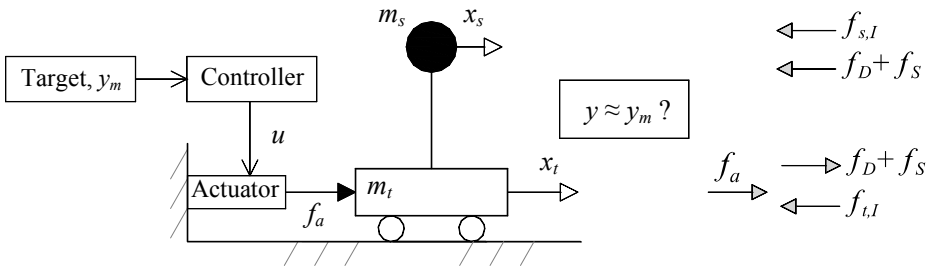

Figure 1. Schematic of a shake table-structure system.

In order to move the structure sitting on the platform to match a target response y_m, a controlled excitation should be applied at its base. The objective of this control system of the shake table–structure is to determine the control excitation input $u(t)$, which is the desired shake table displacement $x_d(t)$ in this study, such that the response output $y(t)$ of the shake table or the mounted structure will follow the pre-defined target motion $y_m(t)$. In order to achieve this goal, a mathematical model of the system is introduced based on the developments by Rinawi and Clough [2] for a shake table-actuator system and Sivaselvan and Reinhorn [13] for a nonlinear hysteretic structure.

Assuming linear relationships between the servovalve input and output oil flow rate, and between the oil flow rate and the servovalve's spool displacement, the relation between the shake table input $u = x_d$ and the output x_t can be expressed in the time domain [1], [2]:

$$k_a x_d(t) = \frac{1}{\omega_a^2}\frac{\dot{f}_a(t)}{m_t} + \frac{2\xi_a}{\omega_a}\frac{f_a(t)}{m_t} + \dot{x}_t(t) + k_a x_t(t) \tag{1}$$

where ω_a, ξ_a, and k_a are the natural frequency, the equivalent damping ratio, and the control gain of the shake table system, respectively. The natural frequency of the shake table system ω_a (rad/s) is

also known as oil column frequency; i.e. $f_{n,a}$ (Hz) = ω_a / 2π = π^{-1} $(\beta A^2/Vm_t)^{0.5}$ [3], in which: A is the actuator piston area; V is the volume of oil in the actuator; β is the bulk modulus of fluid.

Structures (specimens) subjected to strong excitation can experience nonlinear hysteretic behavior due to yielding, or due to the nature of the seismically protected structure such as a base isolated system. A class of smooth hysteretic models was originally proposed by Bouc [14] and modified by many researchers including Wen, Y. K. [15] and Sivaselvan and Reinhorn [13]. Sivaselvan and Reinhorn [13] claim that the restoring force $f_S(\underline{x})$ can be modeled as a combination of elastic and hysteretic components (as expressed in Eq. (3)). Even though the model is versatile and capable to simulate stiffness degradation, strength degradation, and pinching, this study focuses only on a plain, bilinear type hysteretic behavior in order to facilitate the development of a real-time controller.

Considering a nonlinear hysteretic *single degree-of-freedom* (SDOF) system, the equation of motion can be written as (adopted from Sivaselvan and Reinhorn [13]):

$$m_s\ddot{x}_s(t) + c_s\dot{x}_s(t) + f_S(\underline{x}) = -m_s\ddot{x}_t(t) \tag{2}$$

where c_s is the damping of the structure, and $f_S(\underline{x})$ is a nonlinear restoring force. The governing equation of the restoring force is expressed

$$\begin{aligned} &\dot{f}_S(\underline{x}) = \left[\alpha k_s + (1-\alpha)k_H(\underline{x})\right]\dot{x}_s(t) \quad \textit{which is equivalent to}: \\ &df_S(\underline{x})/dx = \left[\alpha k_s + (1-\alpha)k_H(\underline{x})\right] = k_T(\underline{x}) \end{aligned} \tag{3}$$

in which $k_T(\underline{x})$ indicates the instantaneous tangent stiffness; k_s is the elastic stiffness; $k_H(\underline{x})$ is the hysteretic stiffness; and α is the post-yielding stiffness ratio to the elastic stiffness having the following property: $0 < \alpha < 1$. In this parallel-spring representation, the stiffness of the hysteretic spring $k_H(\underline{x})$ can be expressed as

$$k_H(\underline{x}) = k_s\left\{1 - \left[\eta_2 + \eta_1 \operatorname{sgn}\left(f_H(\underline{x})\dot{x}_s(t)\right)\right]\left(\left|f_H(\underline{x})\right| / f_y^*\right)^N\right\} \tag{4}$$

where the hysteretic force $f_H(\underline{x}) = f_S(\underline{x}) - \alpha k_s x(t)$; the hysteretic yielding force $f_y^* = (1-\alpha) f_y$ with the yielding force $f_y = k_s d_y$ where d_y is the yielding displacement; N is the power controlling the smoothness of the transition from elastic to inelastic range; η_1, η_2 are parameters controlling the shape of the hysteretic loop, which must satisfy $\eta_1 + \eta_2 = 1$ [16] i.e. in this study, $\eta_1 = \eta_2 = 0.5$ are chosen for simplicity, and sgn = the *signum function*. The instantaneous tangent stiffness $k_T(\underline{x})$ in Eq. (3) can be rewritten therefore as

$$k_T(\underline{x}) = \alpha k_s + (1-\alpha)k_s\left\{1 - 0.5\left[1 + \operatorname{sgn}\left(f_H(\underline{x})\dot{x}_s(t)\right)\right]\left(\left|f_H(\underline{x})\right| / f_y^*\right)^N\right\} \tag{5}$$

and its response can be fully captured by four constant parameters: k_s, α, d_y, and N; in addition to the knowledge of the state responses. First, assuming that all these parameters are known a priori, a nonlinear feedback controller is proposed in Section 3. However, in real applications, only initial approximations of the true parameters might be available from static tests; therefore in Section 4, a real-time estimator to determine these parameters is introduced to be combined with the controller. It is noted that the control law determined in Section 3 involves the differentiation of the instantaneous stiffness $k_T(\underline{x})$ and the estimator (the extended Kalman filter) in Section 4 requires the Jacobian matrix; however, Eq. (3) includes the terms of $\operatorname{sgn}(\dot{x}_s(t)) \times \dot{x}_s(t) = |\dot{x}_s(t)|$ that is not a differentiable function at $\dot{x}_s(t) = 0$. In this study, $d|x| / dx \triangleq \operatorname{sgn}(x)$; it is defined along with $d|x| / dx \triangleq 0$ at $x = 0$, assuming that this instant effect might be not significant in the control and estimation procedure; this assumption is examined through numerical simulations in Section 5.

Considering a test structure mounted on the shake table shown in Figure 1 is a nonlinear hysteretic SDOF system, the equations of motion of the shake table-structure system can be expressed in the state space form [17], [18]:

$$\dot{\underline{x}}(t) = \underline{f}\left(\underline{x}(t), u(t)\right) \qquad or$$

$$\frac{d}{dt}\begin{bmatrix} x_s(t) \\ \dot{x}_s(t) \\ f_S(\underline{x}) \\ x_t(t) \\ \dot{x}_t(t) \\ f_a(t)/m_t \end{bmatrix} = \begin{bmatrix} \dot{x}_s(t) \\ -\left(m_s^{-1} + m_t^{-1}\right)\left\{c_s\dot{x}_s(t) + f_S(\underline{x})\right\} - m_t^{-1} f_a(t) \\ k_T(\underline{x})\dot{x}_s(t) \\ \dot{x}_t(t) \\ m_t^{-1}\left\{c_s\dot{x}_s(t) + f_S(\underline{x})\right\} + f_a(t)/m_t \\ -k_a\omega_a^2 x_t(t) - \omega_a^2\dot{x}_t(t) - 2\xi_a\omega_a f_a(t)/m_t + k_a\omega_a^2 x_d(t) \end{bmatrix} \tag{6}$$

where $u(t) = x_d(t)$, and ω_a, ξ_a, and k_a are the natural frequency, the equivalent damping ratio, and the control gain of the shake table system as defined in Eq. (1), and all parameters are previously defined. For the output $y(t)$ of the total acceleration response $\ddot{x}_s^{\,t}(t) = \ddot{x}_s(t) + \ddot{x}_t(t)$ at the top of the structure, the output equation is

$$y(t) = -m_s^{-1}\left\{c_s\dot{x}_s(t) + f_S(\underline{x})\right\}. \tag{7}$$

The equation can be solved by using the 4*th* order Runge-Kutta method for actual implementations.

3 TRACKING CONTROL METHOD

For the tracking control of a shake table-nonlinear hysteretic structure system, a nonlinear feedback controller based on the *feedback linearization control* method [8], [9] is proposed. Using the feedback linearization tracking control (FTC), a controller can be designed to cancel undesired nonlinear terms and to introduce a new linear input term such that the output response of the controlled system follows a desired target motion.

The shake table-nonlinear hysteretic structure model, expressed in Eq. (6) and Eq. (7) with the output $y(t)$ of the total acceleration response $\ddot{x}_s^{\,t}(t)$ at the structure, can be rewritten:

$$\begin{cases} \ddot{x}_s(t) + a\dot{x}_s(t) + m_s^{-1} f_S(\underline{x}) = -\ddot{x}_t(t) \\ \ddot{x}_t(t) - \left\{c\dot{x}_s(t) + m_t^{-1} f_S(\underline{x})\right\} = f_a^*(t) \\ \dot{f}_S(\underline{x}) = k_T(\underline{x})\dot{x}_s(t) \\ \dot{f}_a^*(t) + ef_a^*(t) + f\dot{x}_t(t) + gx_t(t) = gu(t) \\ y(t) = -a\dot{x}_s(t) - m_s^{-1} f_S(\underline{x}) \end{cases} \tag{8}$$

by using abbreviated notations for sake of simplification:

$$a = m_s^{-1}c_s; \quad b = m_s^{-1}k_s; \quad c = m_t^{-1}c_s; \quad e = 2\xi_a\omega_a; \quad f = \omega_a^2; \quad g = \omega_a^2 k_a;$$
$$f_a^*(t) = f_a(t)/m_t; \quad u(t) = x_d(t).$$

The system output $y(t)$ is to be differentiated until the control excitation input $u(t)$ appears in the expression of the differentiated output. For this system, after differentiating the output twice, the control excitation input appears

$$\begin{aligned} \ddot{y}(t) = &\left[a(a+c) - m_s^{-1}k_T(\underline{x})\right]\ddot{x}_s(t) + \left[-m_s^{-1}\dot{k}_T(\underline{x}) + a\left(m_s^{-1} + m_t^{-1}\right)k_T(\underline{x})\right]\dot{x}_s(t) \\ &+ (-ae)f_a^*(t) + (-af)\dot{x}_t(t) + (-ag)x_t(t) + agu(t) \end{aligned} \tag{9}$$

where the expression of $\dot{k}_T(\underline{x})$ can be found in [17], [18]. The main objective of the tracking control is to reduce a tracking error signal $e(t) = y(t) - y_m(t)$, which is defined as the difference between the

system output $y(t)$ and the target motion $y_m(t)$, by using the control excitation input $u(t)$. The desired tracking error dynamics can be defined as

$$\ddot{e}(t)+k_1^*\dot{e}(t)+k_2^*e(t)=0 \tag{10}$$

where k_1^* and k_2^* are tracking error design coefficients. It is noted that in order to guarantee the boundedness of all state responses $\underline{x}(t)$ of the controlled system, one may introduce the following additional error terms, as addressed in another work of the authors [17], [18]:

$$e_{add}(t)=k_3^*\left[\dot{x}_s^t(t)-\int_0^t y_m(\tau)d\tau\right]+k_4^*\left[x_s^t(t)-\int_0^t\int_0^\tau y_m(\zeta)d\zeta d\tau\right] \tag{11}$$

where k_3^* and k_4^* are tracking error design coefficients, the total displacement $x_s^t(t) = x_s(t) + x_t(t)$ and the total velocity $\dot{x}_s^t(t) = \dot{x}_s(t) + \dot{x}_t(t)$, and the integration and double integration of the target motion $y_m(t)$ are chosen as bounded motions and their initial values are zeros. The following relations are used in this study:

$$\frac{d}{dt}\left[\dot{x}_s^t(t)-\int_0^t y_m(\tau)d\tau\right]=\underbrace{y(t)-y_m(t)}_{e(t)};\quad \frac{d^2}{dt^2}\left[x_s^t(t)-\int_0^t\int_0^\tau y_m(\zeta)d\zeta d\tau\right]=\underbrace{y(t)-y_m(t)}_{e(t)}. \tag{12}$$

Therefore, by introducing a new term, $\overline{e}(t) = [x_s^t(t) - \int_0^t \int_0^\tau y_m(\zeta)d\zeta d\tau]$, the desired tracking error dynamics (Eq. (10)) with the additional terms in Eq. (11) can be rewritten as

$$\overline{e}^{(4)}(t)+k_1^*\overline{e}^{(3)}(t)+k_2^*\ddot{\overline{e}}(t)+k_3^*\dot{\overline{e}}(t)+k_4^*\overline{e}(t)=0 \tag{13}$$

where $\overline{e}^{(4)}$ and $\overline{e}^{(3)}$ denote the fourth and third derivatives of $\overline{e}(t)$ with respect to time, respectively, and as discussed above, k_1^* through k_4^* are tracking error coefficients.

Equation (13) can be rewritten by using the expression $\overline{e}^{(4)} = \ddot{y}(t) - \ddot{y}_m(t)$ as

$$\left[\ddot{y}(t)-\ddot{y}_m(t)\right]+k_1^*\overline{e}^{(3)}(t)+k_2^*\ddot{\overline{e}}(t)+k_3^*\dot{\overline{e}}(t)+k_4^*\overline{e}(t)=0. \tag{14}$$

Moving all terms in Eq. (14) to the right-hand side except $\ddot{y}(t)$ gives

$$\ddot{y}(t)=\ddot{y}_m(t)-k_1^*\overline{e}^{(3)}(t)-k_2^*\ddot{\overline{e}}(t)-k_3^*\dot{\overline{e}}(t)-k_4^*\overline{e}(t)\ \ or\ \ \upsilon^*(t) \tag{15}$$

where a new term notation $\upsilon^*(t) = \ddot{y}_m(t) - k_1^*\overline{e}^{(3)}(t) - k_2^*\ddot{\overline{e}}(t) - k_3^*\dot{\overline{e}}(t) - k_4^*\overline{e}(t)$ is introduced for brevity. Equating this equation to the right-hand side of Eq. (9) yields

$$\begin{aligned}&\left[a(a+c)-m_s^{-1}k_T(\underline{x})\right]\ddot{x}_s(t)+\left[-m_s^{-1}\dot{k}_T(\underline{x})+a\left(m_s^{-1}+m_t^{-1}\right)k_T(\underline{x})\right]\dot{x}_s(t)\\&\quad+(-ae)f_a^*(t)+(-af)\dot{x}_t(t)+(-ag)x_t(t)+agu(t)=\upsilon^*(t).\end{aligned} \tag{16}$$

By solving this equation for the control excitation input $u(t)$, the feedback tracking control law is obtained as following:

$$u(t)=(ag)^{-1}\left[-\ddot{y}^*(t)+\upsilon^*(t)\right] \tag{17}$$

where the first term $\ddot{y}^*(t)$ is defined from Eq. (9) in order to cancel the original system dynamics as

$$\begin{aligned}\ddot{y}^*(t)=&\left[a(a+c)-m_s^{-1}k_T(\underline{x})\right]\ddot{x}_s(t)+\left[-m_s^{-1}\dot{k}_T(\underline{x})+a\left(m_s^{-1}+m_t^{-1}\right)k_T(\underline{x})\right]\dot{x}_s(t)\\&+(-ae)f_a^*(t)+(-af)\dot{x}_t(t)+(-ag)x_t(t)\end{aligned} \tag{18}$$

and the new input $\upsilon^*(t)$ in Eq. (17) is chosen to accomplish the tracking objective as expressed in Eq. (15).

By using the control excitation input determined above, $u(t)$ in Eq. (17), it is ensured that the tracking error $e(t) \to 0$ as $t \to \infty$ as shown in Eq. (13) (i.e. $e(t) = \ddot{\overline{e}}(t)$ as in Eq. (12)). It is noted that

the tracking error coefficients, k_1^* through k_4^* in Eq. (13), can be chosen by the engineer to achieve desired responses; i.e. for example, one may choose 2 of the four eigenvalues for a dominant second-order system and choose the remaining eigenvalues to have a sufficiently damped response, as in an estimator design approach [12], such that all eigenvalues of the system matrix corresponding to Eq. (13) have negative real parts; thus, the tracking error terms $\underline{\bar{e}}(t) = [\bar{e}, \dot{\bar{e}}, \ddot{\bar{e}}, \bar{e}^{(3)}]^T$ will go to zero as time goes to infinity; $\underline{\bar{e}}(t) \rightarrow 0$ as $t \rightarrow \infty$.

In order to check the boundedness of the state responses $\underline{x}(t)$ of the controlled system, one may check the closed loop system by substituting the control excitation input $u(t)$ from Eq. (17) into the true system equation shown in Eq. (8). It has been shown that if the target $y_m(t)$ and its derivatives ($\dot{y}_m(t)$, $\ddot{y}_m(t)$) and its integration and double integration as in Eq. (12) are bounded and the design coefficient is $k_1^* \geq c_s(m_s^{-1}+m_t^{-1})$, the all state responses $\underline{x}(t)$ are bounded. The interested reader is referred to the work of the authors [17].

4 STATE AND PARAMETER ESTIMATION METHOD

When system properties are not fully known, it is essential to identify and quantify these system parameters for the tracking control problem. The *extended Kalman filter* (EKF), well-known system state and parameter identification method [10], [11], is adopted in this study. A general formulation of the EKF can be found in the previous studies [10], [12]. In addition to the true state estimation $\underline{x}$ from the measurements that are contaminated by noise, the EKF can be also used to estimate unknown system parameters $\underline{\theta}$. In order to estimate system parameters, new states are augmented to the original state vector i.e. $\underline{x}_a(t) = [\underline{x}^T(t) \quad \underline{\theta}^T]^T$. For the shake table-nonlinear hysteretic structure system, $\underline{x}(t) = [x_s(t) \;\; \dot{x}_s(t) \;\; f_S(\underline{x}) \;\; x_t(t) \;\; \dot{x}_t(t) \;\; f_a(t)/m_t]^T$ (refer to Eq. (6)) and $\underline{\theta} = [c_s \;\; k_s \;\; \alpha \;\; d_y \;\; N]^T$; thus, the dimension of the augmented state vector becomes $n = 11$ in this case. It is noted that the four constant parameters: k_s, α, d_y, and N; are needed to estimate the instantaneous stiffness $k_T(\underline{x})$ (refer to Eq. (5)). The performance of the estimator with uncertainties in model parameters and in measurements is demonstrated by the numerical simulations in Section 5.

5 NUMERICAL SIMULATION OF ADAPTIVE CONTROL

For a nonlinear structure with known parameters mounted on a shake table, the tracking control law is established as shown in Eq. (17) in Section 3. When there are uncertainties in the system model parameters, one possible way is to use the adaptive control scheme that combines the established control law with the estimated parameters using the real-time estimator introduced in Section 4. For the case where the damping coefficient c_s and the instantaneous stiffness $k_T(\underline{x})$ of the test structure are not fully known, five constant system parameters $\underline{\theta} = [c_s \;\; k_s \;\; \alpha \;\; d_y \;\; N]^T$ are to be estimated as discussed in Section 4. The established control law in Eq. (17) can be reformulated by using the estimated values: $\hat{c}_s(t)$, $\hat{k}_T(\underline{x})$ (i.e. *hat* ^ indicates the estimated parameters); of the true parameters: c_s, $k_T(\underline{x})$; as well as the estimated state responses $\underline{\hat{x}}(t)$. Due to estimation errors, the right-hand side of the tracking error dynamic equation in Eq. (13) may have some residual errors. The tracking error $e(t)$ will diminish when the estimated error becomes small. As discussed in Section 3 above, the tracking error coefficients k_1^* through k_4^* can be chosen to achieve desired responses by the engineer. It is noted, however, that the demand of faster tracking performance may require larger control efforts and may cause a problem in the stability of the controller.

The feedback tracking control method combined with the real-time state and parameter estimator using the EKF is applied to a realistic shake table and structure system whose characteristics are obtained from the real systems in the Structural Engineering and Earthquake Simulation Laboratory (SEESL) at the University at Buffalo (UB). Numerical simulations are

performed for practical target motions generated from selected excitation motions including a real earthquake motion.

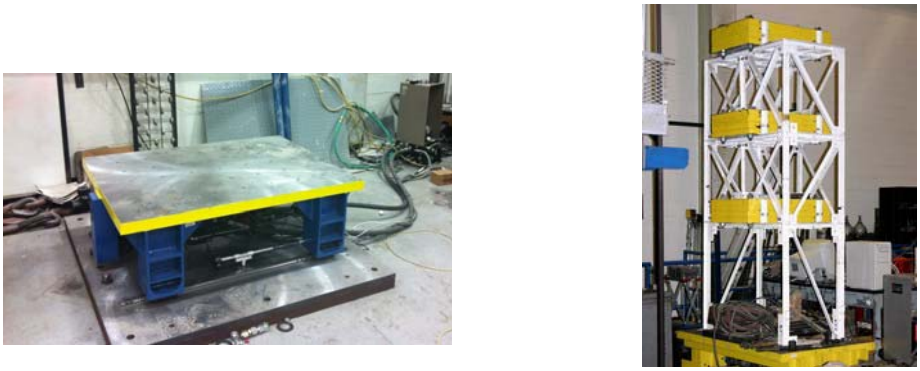

Figure 2. UB uniaxial shake table [19] (left) and an SDOF structure [20] (right).

The shake table consists of one uniaxial actuator having the maximum horizontal actuator force $f_{a,max}$ = 24.5 kN and stroke $x_{t,max}$ = 76 mm and a 1219 × 914 mm platform, whose mass m_t = 1,589 kg, as shown in Figure 2 (left) [19]. The natural frequency $f_{n,a}$, the equivalent damping ratio ξ_a, and the control gain k_a of the shake table system defined in Eq. (1) are $f_{n,a}$ = 30 Hz, ξ_a = 50 %, k_a = 25 where the values of ξ_a and k_a are assumed in this numerical study.

The structure, shown in Figure 2 (right), is a three-story steel frame shear building rigidly braced in the top two floors to simulate an SDOF system [21]. The mass of the structure m_s = 2950 kg; the structure elastic stiffness k_s = 1.4 kN/mm; damping coefficient c_s = 0.0016 kN·sec/mm; i.e. therefore, (before yielding) the fundamental frequency $f_{n,s}$ = 3.47 Hz and the inherent damping ratio ξ_s = 1.24 %. The yielding force f_y = 24.9 kN, and post-yielding stiffness ratio to the elastic stiffness α = 0.1 are chosen to demonstrate the hysteresis behavior effects on the tracking control in this study. It is noted that the dynamic properties of a shake table such as ω_a, ξ_a, and k_a: the natural frequency, the equivalent damping ratio, and the control gain of the shake table system, respectively; are subject to change after mounting a test structure on the shake table because of the shake table-structure interaction. Therefore, it is necessary to identify them at the beginning of testing using quasi-static and/or dynamic system identification procedures as described in [2], [22]. In this numerical simulation, the aforementioned shake table properties are used.

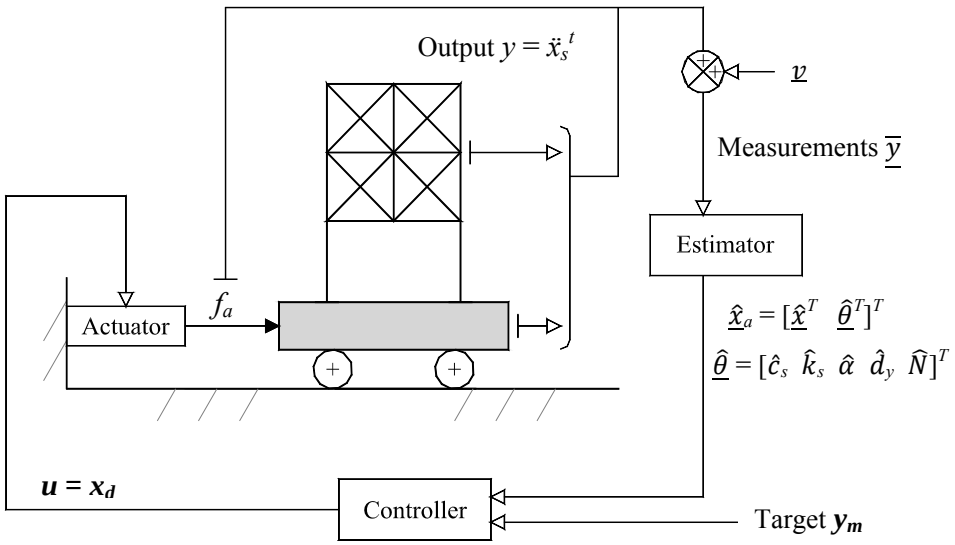

Figure 3. Tracking control setup for an SDOF nonlinear system using a shake table.

Figure 3 shows the schematic of the tracking control test setup for the shake table-structure. The target motion $y_m(t)$ is pre-defined according to test objectives. The output response $y(t) = \ddot{x}_s^t(t)$, the total acceleration of the top of the test structure. The control excitation input $u(t)$ (i.e. $u(t) = x_d(t)$, the desired shake table displacement in this study), is computed by using the tracking control method (refer to Eq. (17)) with the measurements from instrument sensors. For practical applications, instead of the full state $\underline{x}(t) = [x_s(t) \;\; \dot{x}_s(t) \;\; f_S(\underline{x}) \;\; x_t(t) \;\; \dot{x}_t(t) \;\; f_a(t)/m_t]^T$ feedback, limited measurements including the structure displacement $x_s(t)$ and total acceleration $\ddot{x}_s^t(t)$, and the table displacement $x_t(t)$ and actuator force $f_a(t)$ are considered; i.e. $\underline{\overline{y}}_k = [\overline{x}_{s,k} \;\; \ddot{\overline{x}}_{s,k}^t \;\; \overline{x}_{t,k} \;\; \overline{f}_{a,k}/m_t]^T$, where *bar* ($\bar{}$) indicates the measured responses. In order to examine the measurement noise effects, a zero-mean Gaussian white-noise process of 3% RMS noise-to-signal ratio are added to each measurement. Five unknown parameters $\underline{\theta} = [c_s \;\; k_s \;\; \alpha \;\; d_y \;\; N]^T$ are to be estimated. The *extended Kalman filter* (EKF) is used to estimate the unknown parameters and the true state responses from the measurements contaminated by noise as described in Section 4.

The tracking control results using the *feedback linearization tracking control* (FTC) method combined with the *extended Kalman filter* (EKF) estimator are obtained through numerical analyses; some of the interesting results are presented below. The selected control parameters are $k_1^* = 42$, $k_2^* = 592$, $k_3^* = 4{,}200$, $k_4^* = 10{,}000$ (see Eq. (13)) by assigning the dynamic characteristics of the tracking error equation to be $\omega_{e1} = 10$, $\xi_{e1} = 0.7$ and $\omega_{e2} = 10$, $\xi_{e2} = 1.4$. For the parameter estimations using the EKF, the initial parameter estimate $\underline{\hat{\theta}}_0$ is chosen as $\underline{\hat{\theta}}_0 = 0.8 \times \underline{\theta}^*$ (20% errors in the initial guesses), and the initial covariance matrix is chosen as $P_0 = \text{diag}([0 \;\; 0 \;\; 0 \;\; 0 \;\; 0 \;\; 0 \;\; \hat{c}_{s,o}^{\,2} \;\; \hat{k}_{s,o}^{\,2} \;\; \hat{\alpha}_o^{\,2} \;\; \hat{d}_{y,o}^{\,2} \;\; \hat{N}_o^{\,2}]^T \times 0.01)$. The error covariance matrices Q_E and R_E are chosen as $Q_E = 0 \times I_{11\times 11}$ (i.e. all zeroes, assuming the errors in the system model is negligible) and the R_E = diagonal matrix, whose elements are computed as the square of noise *root-mean-square* (RMS); i.e. noise RMS = 3% × corresponding signal RMS (i.e. noise variances R_E are assumed to be known from the instruments information). The time step of 0.002 sec (sampling rate = 500 sec^{-1}) is used for the simulations. The target motion $y_m(t)$ is the total acceleration output, generated from a reference linear SDOF system. The linear reference system properties are: $m_m = 2950$ kg, $k_m = 2.9$ kN/mm, and $c_m = 0.0093$ kN·sec/mm ($f_{n,m} = 5.0$ Hz, $\xi_m = 0.05$), subjected to a real earthquake motion, Elcentro N-S, 1940 100% [23], which is high-pass filtered at 0.3 Hz cutoff frequency in order to avoid large demand of shake table shift. The target motion is presented in Figure 4 (a - Target). The tracking control results are presented in Figure 4 through Figure 9.

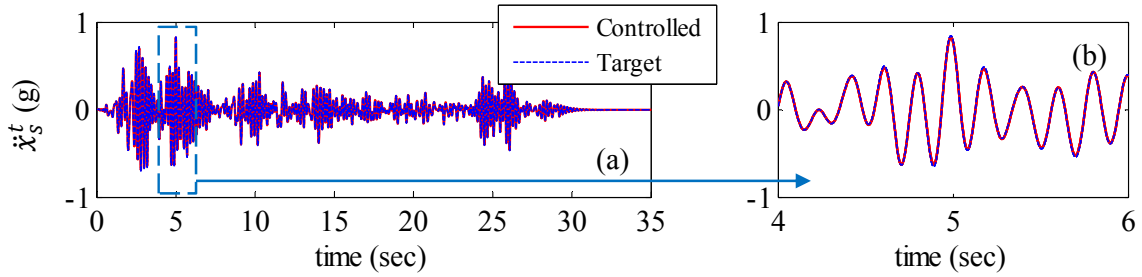

Figure 4. Target vs. Controlled total acceleration: (a) 0 - 35 sec; (b) Zoomed view 4 – 6 sec.

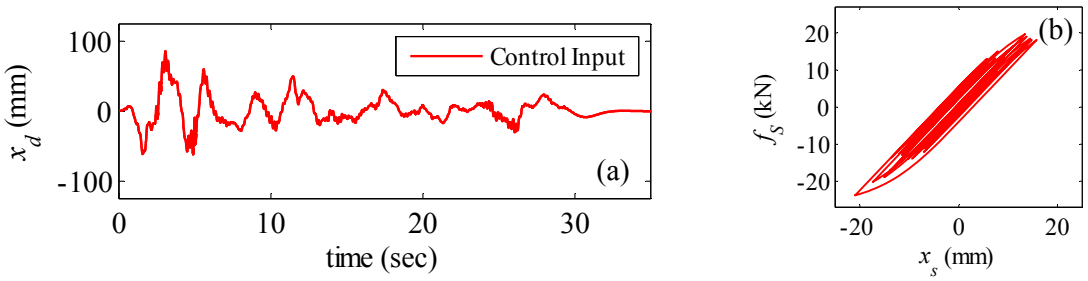

Figure 5. (a) Control input ($u = x_d$); (b) Structure restoring force f_S - displacement x_s relationship.

Figure 4 presents the comparisons between the target motion $y_m(t)$ and the controlled output of the total acceleration at the top of the structure $y(t) = \ddot{x}_s^t(t)$, and they show very good agreements. Figure 5 (a) presents the control excitation input $u(t) = x_d(t)$, the desired shake table displacement. The structure restoring force $f_S(\underline{x})$ and the relative displacement $x_s(t)$ relationship is shown in Figure 5 (b). Figure 6 presents the performance of the system parameter estimation of the five constant parameters $\underline{\theta} = [c_s \;\; k_s \;\; \alpha \;\; d_y \;\; N]^T$. The results show good convergence to the true values (i.e. note that the initial guess of each parameter has 20% error as addressed above); i.e. the estimated errors = |true - estimated| / true × 100% are between 0.1% and 3.8% (the estimated values are identified at the end of each history). Figure 7 presents the comparisons between the true vs. estimation of the instantaneous stiffness $k_T(\underline{x})$, determined by using the estimated constant parameters of k_s, α, d_y, and N (refer to Eq. (5)), and shows very good agreements: it is a very encouraging result because the accuracy of the instantaneous stiffness $k_T(\underline{x})$ for the control excitation computation (refer to Eq. (17)) is more important than that of each constant parameter.

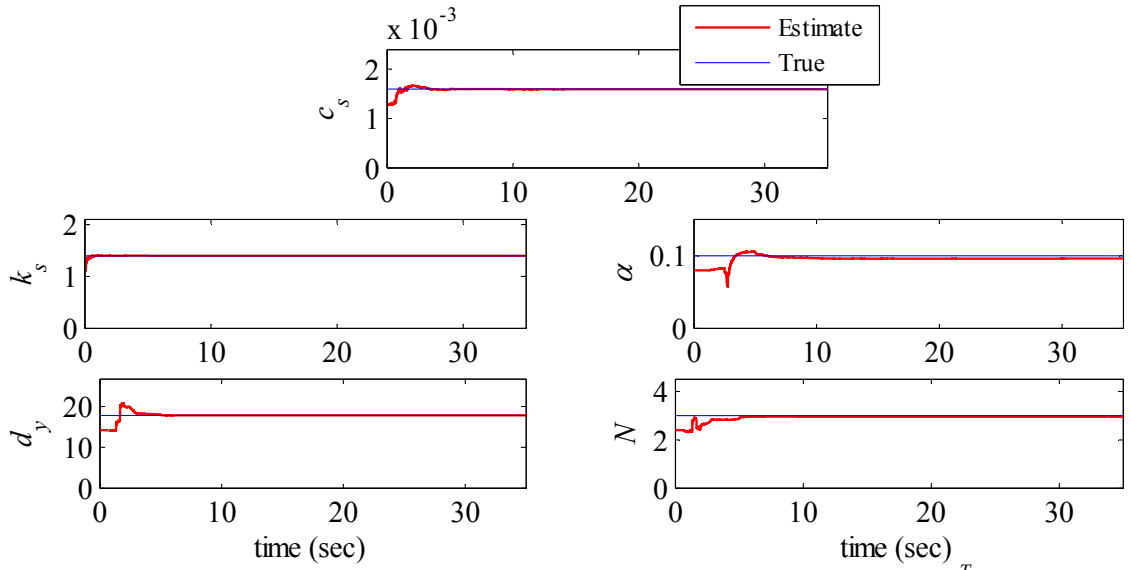

Figure 6. Estimate of constant parameters $\underline{\theta} = [c_s \;\; k_s \;\; \alpha \;\; d_y \;\; N]^T$.

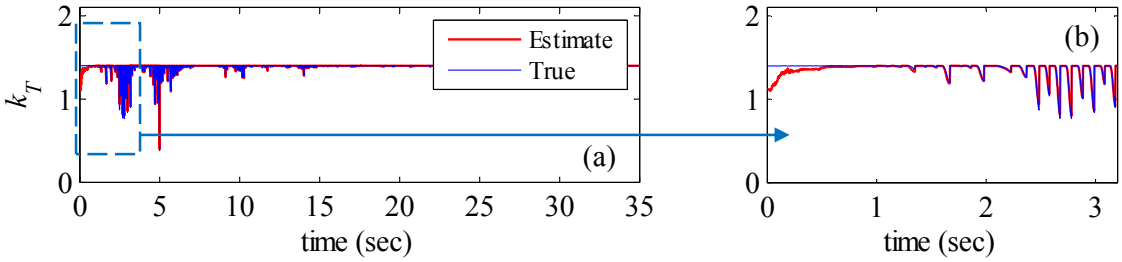

Figure 7. Estimate of instantaneous stiffness $k_T(\underline{x})$: (a) 0 - 35 sec; (b) Zoomed view 0 – 5.5 sec.

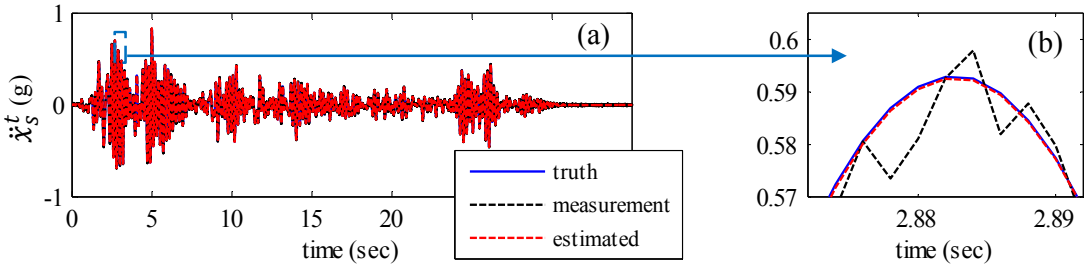

Figure 8. Estimate of structure total acceleration $\ddot{x}_s^t(t)$:(a) 0-35 sec; (b)Zoomed view 2.87–2.89 sec.

Figure 8 presents the comparison between the estimated and measured structure total acceleration responses $\ddot{x}_s^t(t)$, where the estimated response is computed by using the estimated state responses as expressed in the last equation of Eq. (8). The results clearly show that the measurement noise is effectively reduced by the EKF.

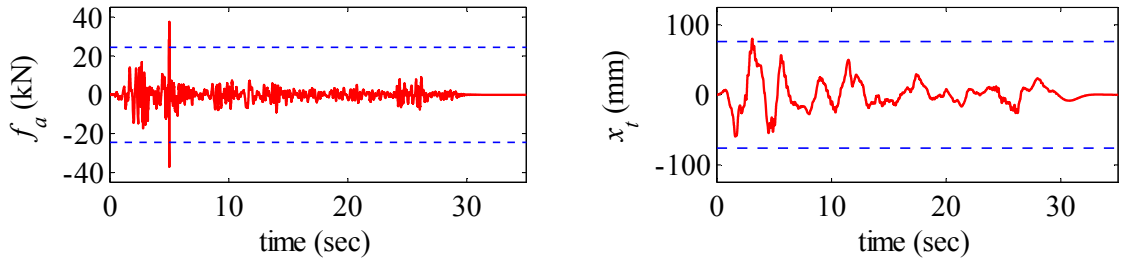

Figure 9. Shake table response: (a) Actuator force $f_a(t)$; (b) Table displacement $x_t(t)$.

Although the tracking performance is very good and all responses of the controlled system are bounded, Figure 9 indicates that the force $f_a(t)$ capacity demend of the actuator and shake table displacement $x_t(t)$ (shown by the blue dot lines) are exceeded. Thus the simulation reveals the limitation of the testing system. This limitation might be overcome by adjusting the target motion and/or the properties of the test structure and shake table. In this study, the target motion is reduced by 20% (as usually done for practical purposes in laboratory when the equipment has limitations): in other words, a new target motion is generated from the same linear reference model subjected to Elcentro N-S 80% excitation. As expected, using the reduced amplitude of the target motion, the maximum actuator force demand and the table displacement are $f_{a,max}$ = 16 kN and $x_{t,max}$ = 65 mm, which are within the allowable limits. The results of the simulation for the reduced amplitude target motion shows that the agreement between the target motion and the controlled output is very good as in the previous example. It is noted that the reducing the test demand (the target motion) requires smaller restoring force and structural deformation, such that less nonlinear hysteretic behavior occurs and results in smaller responses of the shake table.

Instead of reducing the amplitude of the target motion, the test structure can be also mounted on a larger shake table. For example, the maximum actuator force and table displacement of the 6DOF shake table at the University at Buffalo are 225 kN and 150 mm, respectively [24], which are greater than the maximum demands of actuator force (38 kN) and table displacement (80 mm) (presented in Figure 9). Since the system responses will be affected by the dynamics of the shake table, the feasibility of applications will need to be checked again by using the simulation procedure developed here. The numerical simulations using the realistic test setup demonstrate that the proposed nonlinear feedback tracking control algorithm can successfully simulate target motions within nonlinear structures experiencing hysteretic behavior. The simulation procedure developed in this study can be used in order to check the limitations and feasibility of applications before actual tests.

6 CONCLUDING REMARKS

For qualification tests using shake tables, whose main objective is to verify certain performance of test structures or equipment, it is often required to challenge the specimens by specified target motions. In these tests, the fidelity of signal reproduction is very important. In this study, a nonlinear feedback tracking controller based on the *feedback linearization control* scheme is proposed to simulate target motions at specific locations of specimens that experience nonlinear behavior. To account for the uncertainties in system parameters and the effects of measurement noise, a real-time state and parameter estimator using the *extended Kalman filter* is adopted and combined with the proposed controller. For practical applications, limited measurements are also

considered. The proposed adaptive control method is applied to a simulation of a realistic test setup including a nonlinear test structure and shake table of the University at Buffalo's laboratory by means of numerical simulations. The results demonstrate that realistic target floor motions, induced by an earthquake motion, can be accurately simulated by using the proposed control method. An experimental study by using the test setup presented in Section 5 is planned in the near future in order to resolve implementation challenges and to study effects of uncertainties.

ACKNOWLEDGEMENT

The work was supported by the Multidisciplinary Center of Earthquake Engineering Research (MCEER) and the Structural Engineering and Earthquake Simulation Laboratory (SEESL) at the University at Buffalo. Financial support was provided by the MCEER Suspended Nonstructural Component Systems Consortium, by the Bonneville Power Administration and by the SEESL administrators. All support is greatly appreciated.

REFERENCES

[1] Blondet, M. & Esparza, C. Analysis of shaking table-structure interaction effects during seismic simulation tests. *Earthquake Engineering and Structural Dynamics* 1988; **16**(4): 473-490.

[2] Rinawi, A. M. & Clough, R. W. Shaking table–structure interaction. *EERC Report No. 91/13*, Earthquake Engineering Research Center, University of California at Berkeley, CA, 1991.

[3] Conte, J. P. & Trombetti, T. L. Linear dynamic modeling of a uniaxial servo-hydraulic shaking table system. *Earthquake Engineering and Structural Dynamics* 2000; **29**(9): 1375–1404.

[4] Reinhorn, A. M. & Ryu, K. P. Maddaloni G. Modeling and Seismic Evaluation of Nonstructural Components: Testing Frame for Experimental Evaluation of Suspended Ceiling Systems. *Technical Report MCEER-10-0004*, Buffalo, NY, 2010.

[5] IEEE Standard 693-2005. IEEE Recommended Practice for Seismic Design of Substations. 2006.

[6] Maddaloni, G., Ryu, K. P. & Reinhorn, A. M. Simulation of floor response spectra in shake table experiments. *Earthquake Engineering and Structural Dynamics* 2010; **40**(6): 591–604. DOI: 10.1002/eqe.1035.

[7] Chen, C. T. *Linear System Theory and Design* (3rd edn). Oxford University Press, NY, 1999.

[8] Slotine, J. J. E. & Li, W. *Applied Nonlinear Control*, Prentice Hall, 1991.

[9] Ioannou, P. A. & Fidan, B. *Adaptive Control Tutorial*. SIAM, Pennsylvania, 2006.

[10] Yun, C. B. & Shinozuka, M. Identification of nonlinear structural dynamic systems. *Journal of Structural Mechanics* 1980; **8**(2), 187–203.

[11] Wu, M. & Smyth, A. W. Application of the unscented Kalman filter for real-time nonlinear structural system identification. *Structural Control and Health Monitoring* 2007; **14** (7): 971–990. DOI: 10.1002/stc.186.

[12] Crassidis, J. L. & Junkins, J. L. *Optimal Estimation of Dynamic Systems* (2nd edn). CRC Press, NY, 2012.

[13] Sivaselvan, M. V. & Reinhorn, A. M. Hysteretic models for deteriorating inelastic structures. *Journal of Engineering Mechanics* 2000; **126**(6): 633–640.

[14] Bouc, R. Forced Vibration of Mechanical System with Hysteresis. *Proc., 4-th Conf. on Non-Linear Oscillations*, 1967.

[15] Wen, Y. K. Methods for Random Vibration of Hysteretic Systems. *Journal of Engineering Mechanics* 1976; **102**(2): 249-263.

[16] Constantinou, M. C. & Adnane, M. A. Dynamics of soil-base-isolated-structure systems evaluation of two models for yielding systems. *Report*, National Science Foundation, 1987.

[17] Ryu, K. P. & Reinhorn, A.M. Real Time Control of Shake Tables for Nonlinear Hysteretic Systems. *Technical Report MCEER-16-0004*, University at Buffalo, Buffalo, NY, 2016, (in print).

[18] Ryu, K. P. & Reinhorn, A.M. Real-Time Control of Shake Tables for Nonlinear Hysteretic Systems. *Structural Control and Health Monitoring* 2016. DOI: 10.1002/stc.1871. (accepted on-line).

[19] Stefanaki, A. A Simple Strategy for Dynamic Substructuring and its Application to Soil-Foundation-Structure Interaction. PhD dissertation, University at Buffalo, Buffalo, NY, 2016, (under review).

[20] UB-SEESL. Lab Manual. <http://nees.buffalo.edu/docs/labmanual/html>, April 21, 2015.

[21] Chung, L. L., Lin, R. C., Soong, T. T. & Reinhorn, A. M. Experimental study of active control for MDOF seismic structures. *Journal of Engineering Mechanics* 1989; **115**: 1609-1627.

[22] Bracci, J. M., Reinhorn, A. M. & Mander, J. B. Seismic Resistance of Reinforced Concrete Frame Structures Designed Only for Gravity Loads - Part I: Design and Properties of a 1/3 Scale Model Structure. *Report NCEER-92-0027*, University at Buffalo, Buffalo, NY, 1992.

[23] Vibrationdata. El Centro Earthquake. <http://www.vibrationdata.com/elcentro.htm>, April 20, 2015.

[24] Reinhorn, A. M., Ryu, K. P. & Pitman, M. Shake Table Testing for Seismic Certification of Suspended Ceiling Systems: System CM1104A of Chicago Metallic Corporation. *Report No UB CSEE/SEESL-2011-08*, University at Buffalo, NY, 2011.